

**The 1987 Reciprocal Tomography Experiment (RTE):
Barotropic Current Data from the Triangular Tomographic Array**

Brian D. Dushaw

*Applied Physics Laboratory, University of Washington, 1013 N.E. 40th St., Box 355640, Seattle,
WA, USA 98105-6698*

June 5, 2026

*Citation: Dushaw, B. D., 2026: The 1987 Reciprocal Tomography Experiment (RTE):
Barotropic Current Data from the Triangular Tomographic Array. Zenodo, 12 pp.,
<https://doi.org/10.5281/zenodo.20535627>*

Corresponding author: Brian Dushaw, dushaw@uw.edu

11 ABSTRACT: The 1987 Reciprocal Tomography Experiment (RTE87) was a test of reciprocal
12 acoustic transmissions over O(1000-km) range for tomographic measurements. The experiment
13 was conducted over summer 1987, with a record length of about 120 days. The triangular
14 tomography array, located some 2000-km north of the Hawaiian Islands, had path lengths 750
15 km (zonal), 1000 km (meridional), and 1250 km. Using acoustic rays that cycle throughout the
16 water column, tomography proved to be ideal for measuring barotropic (depth-averaged) current.
17 The measurements represent a depth- and path-average of current variability, dominated by the
18 barotropic currents, of course. The tomographic measurements of barotropic current were shown
19 to be remarkably accurate. Measurement uncertainties are dominated by geophysical variations,
20 rather than inherent uncertainties, which are likely less than 1 mm/s. The measurements of the
21 barotropic tidal currents agree remarkably well with estimates derived independently from global
22 tidal models. The time series includes all frequencies, from low-frequency current variations of O(5
23 mm/s) to tidal variations of O(20 mm/s). Since the experiment was conducted during the quiescent
24 summer period, low-frequency (< 1 cpd) variations were weak. The current measurements obtained
25 on three sides of a triangle form a measurement of areal-averaged relative vorticity. This publication
26 makes available the tomographic estimates for the time series of barotropic currents derived from
27 the three paths of the tomography array. They are provided for those interested in accurate in situ
28 measurements of low-frequency barotropic current, as well as in situ measurements of barotropic
29 tidal current. Data for the mode-1 internal-tide amplitudes derived from this same experiment are
30 available separately.

1. Barotropic Currents

In 1987 during the Reciprocal Tomography Experiment (RTE87) in the central North Pacific (Figure 1, Table 1), ocean acoustic tomography was tested as a measurement of barotropic currents (Figure 2, [Dushaw et al. \(1994, 1995\)](#)). The triangular tomographic array was deployed during Summer 1987, from about yearday 140 to yearday 260, with record length about 112 days. Acoustic transmissions were made on every fourth day at two hour intervals, hence there were twelve transmissions on a transmission day. The archived time series of barotropic current are unfiltered in time. The triangular array was a right triangle, consisting of a zonal path of about 750-km range, a meridional path of about 1000 km range, and diagonal path of about 1250 km range.

The current measurements were depth- and path-averages, averaged over the acoustic ray paths and along the acoustic paths. The depth-averaging nature of the acoustical observations made for a natural filter barotropic (depth-averaged) variations, other variability, such as from higher-order modes, has near-zero vertical average.

TABLE 1. RTE87 tomography mooring positions

Mooring	Longitude (°W)	Latitude (°N)	Transceiver Depth
1	-157.140626	40.444618	675
2	-157.111321	31.473091	909
3	-165.929733	40.467537	856

This small archive of data from the 1987 experiment required a bit of data archaeology, with the original directory structure for the analysis of the 1995 paper recovered from a 30-year-old compact disk. To the best of my knowledge, the time series in the netcdf file archive are identical to those reported by [Dushaw et al. \(1994, 1995\)](#). The data available for download are the estimated barotropic currents derived from each path of the tomography array ([Dushaw et al. 1994, 1995](#)). The values represent the barotropic current as averaged over the acoustic paths; the time series are dominated by tidal variations.

Figure 2 shows the three time series for barotropic current estimated from each acoustic path. The time series is dominated by tidal variability, with smaller low-frequency variations. The low-frequency variations, of magnitude a few mm/s, are more apparent after computing a daily average

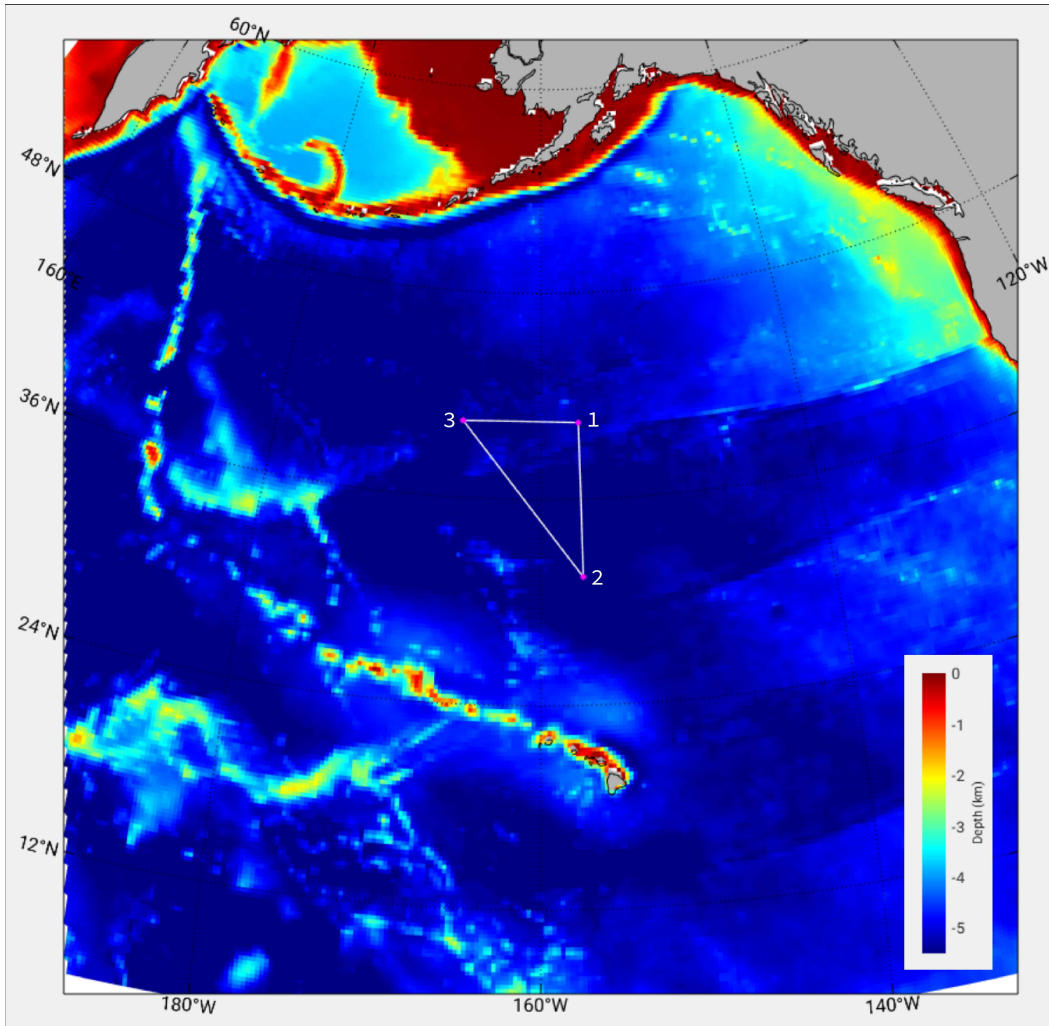


FIG. 1. The triangular array of the 1987 Reciprocal Tomography Experiment in the central North Pacific (Dushaw et al. 1994, 1995). The array has path lengths 750 km (northern zonal path), 1000 km (eastern meridional path), and 1250 km (western path). The labeling numbers for the mooring transceivers are indicated.

of currents (Figure 3). The high-frequency variations (Figure 4) are dominated by tidal variability, as demonstrated by tidal analyses of the time series (Figure 4, blue dotted line). Current along each path has a sign, of course. The convention is positive current is eastward for path (3,1), northward for path (2,1), and northwestward for path (2,3), where, for example, (3,1) means the path from mooring 3 to mooring 1.

The low-frequency barotropic current variations were used to compute the areal-averaged relative vorticity (Dushaw et al. 1994), averaged over the area of the RTE87 triangle. The current variations

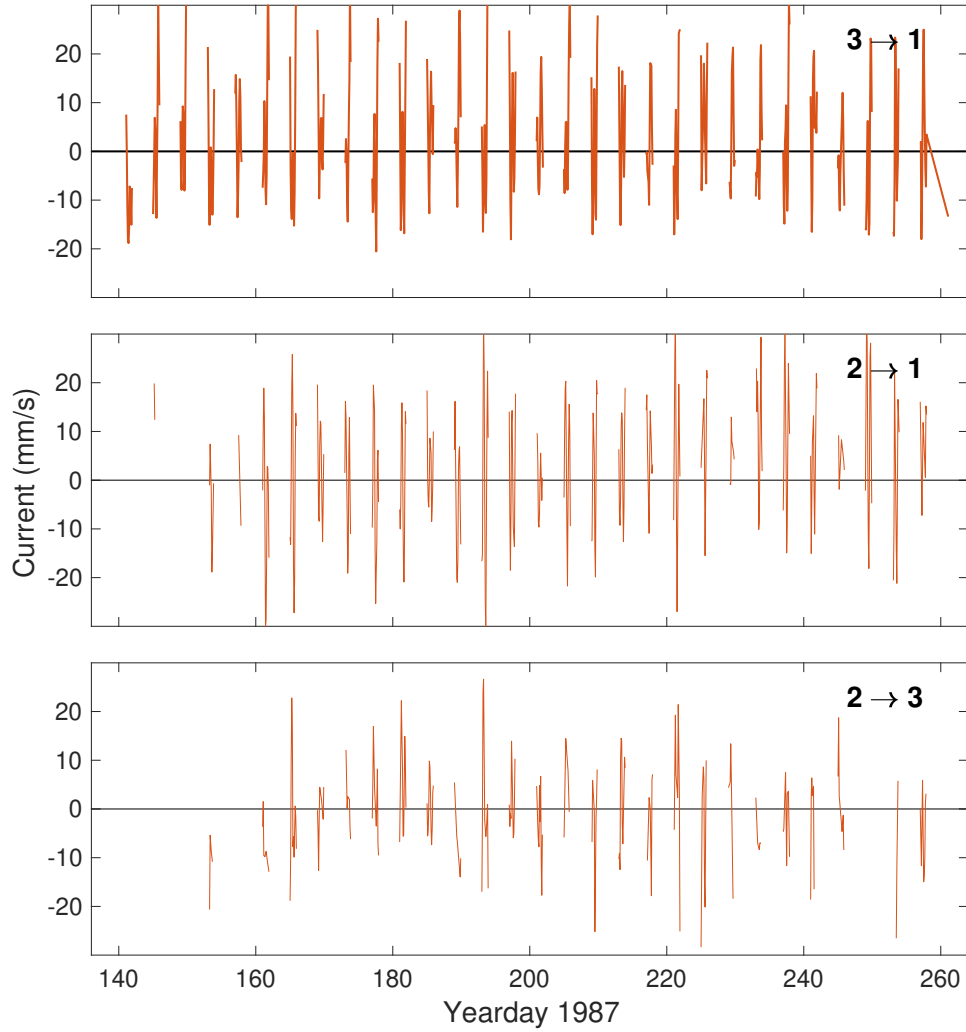


FIG. 2. Timeseries of barotropic (depth-averaged) current derived on the three acoustic paths of the RTE87 experiment. At the upper right of each panel, the acoustic paths are indicated, together with the current direction, with 1 being the northeasternmost mooring, mooring number increasing clockwise around the array. Path 3→1 is a zonal path, path 2→1 is a meridional path. To make the most of limited battery energy, the sampling consisted of twelve acoustic transmissions occurring on every fourth day. The variations are dominated by clear tidal variations, with additional small contributions from low-frequency variations. The tomography measurements were first reported in [Dushaw et al. \(1994\)](#).

on each leg of the triangle may appear random, but they are not. A significant fraction of the variabilities present in the three time series of current cancels in the calculation of vorticity.

Since the tomographic measurements are inherently range and depth averaging, they are nearly ideal measures of barotropic tidal currents (Dushaw et al. 1994, 1995, 1997). The barotropic tidal current harmonic constants derived from tomography have been compared to several global tidal models, highlighting such data as a test for ocean tidal models (Stammer and Coauthors 2014).

This data archive makes the estimated time series for high-frequency barotropic current measured by the RTE87 tomography array available (Dushaw 2026a).

As an aside, the sum of the reciprocal travel times from RTE87 were used to estimate the mode-1 internal tides Dushaw et al. (1995). These observations were interpreted as resulting from internal-tide radiation from the Hawaiian Ridge, some 2000 km to the south. Dushaw et al. (2011); Dushaw (2015b,a) derived estimates for the signals of the mode-1 internal tides from the sea surface height (SSH) data of TOPEX/Poseidon altimetry. Those SSH estimates were used to predict the signals observed during RTE87, or, conversely, the estimates were tested against the in situ tomography measurements, with excellent agreement. The tidal signals obviously dominated the measurements of both barotropic currents and mode-1 temperature. The measurements from the RTE87 experiment of mode-1 internal tides are available separately (Dushaw 2026b).

To highlight the possibilities for which these data may be used, Dushaw and Menemenlis (2023) used the AMODE tomographic time series to test the barotropic tidal current and internal tides of a recent high-resolution ocean model, showing that data from 1991 could be used to predict model internal-tide variability 30 years later in 2020. The model was then used to provide a more accurate picture of the resonant diurnal internal tides described by Dushaw and Worcester (1998). Modelers of barotropic tides go to great lengths to acquire bottom pressure data to test their models. These tomographic measurements provide the same ground truth in tidal current as pressure data do to elevation. Estimated tidal harmonic constants for these time series were published in Dushaw et al. (1995).

2. Barotropic currents from tomography

Estimation of the barotropic currents from acoustic travel times requires an “inverse” computation, or a least-squares fit of the data to a suitable ocean model. A brief sketch is given here; details of the inverse computation can be found in Dushaw et al. (1994). For tomography, we require a linear oceanographic representation for δc or u in terms of known functions and associated scalar

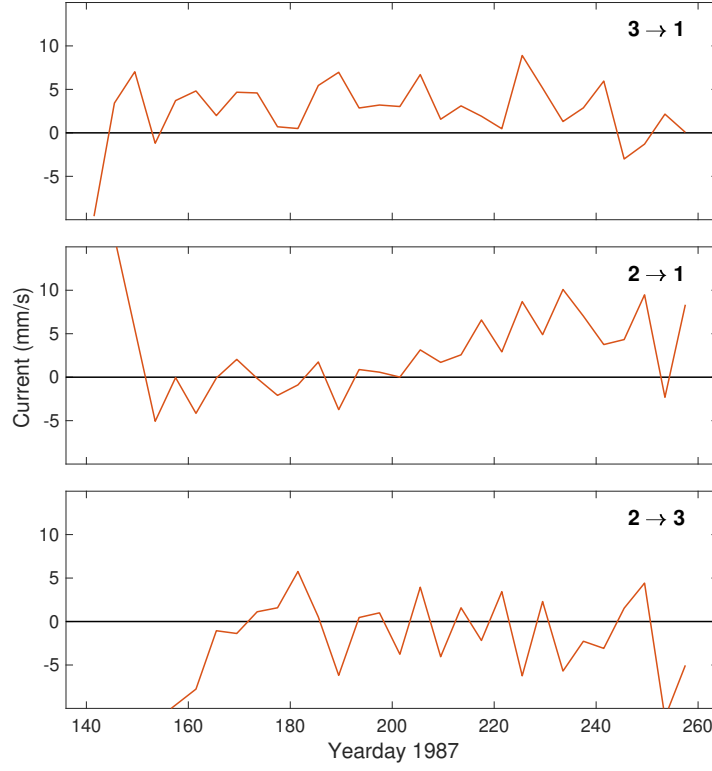


FIG. 3. After computing a daily average, the low-frequency current variations were obtained. Compare with Figure 6 of [Dushaw et al. \(1994\)](#). The figures are not identical, because this recent filtering process is not identical to that used for the 1994 paper.

amplitudes to be estimated. That is, if $F(z)$ is the ocean state of a scalar variable such as sound speed or current along the path to be estimated, then it can be modeled as a linear superposition of one-dimensional functions of depth z ,

$$F(z) = \sum_{n=1}^N A_n P_n(z) \quad (1)$$

where the sum is over the index of vertical functions (P_n). The A_n 's are the amplitudes associated with the vertical functions; they are the parameters to solve for in the inverse.

If $F(z)$ is the current, then the vertical functions $P_n(z)$ are a set of functions that can reasonably be used as a basis set to model current variations in the vertical. The choice of those functions is outside the scope of this document. For the RTE87 environment, only a limited set of acoustic rays were available, and they cycled over the water column. That meant that very little depth resolution

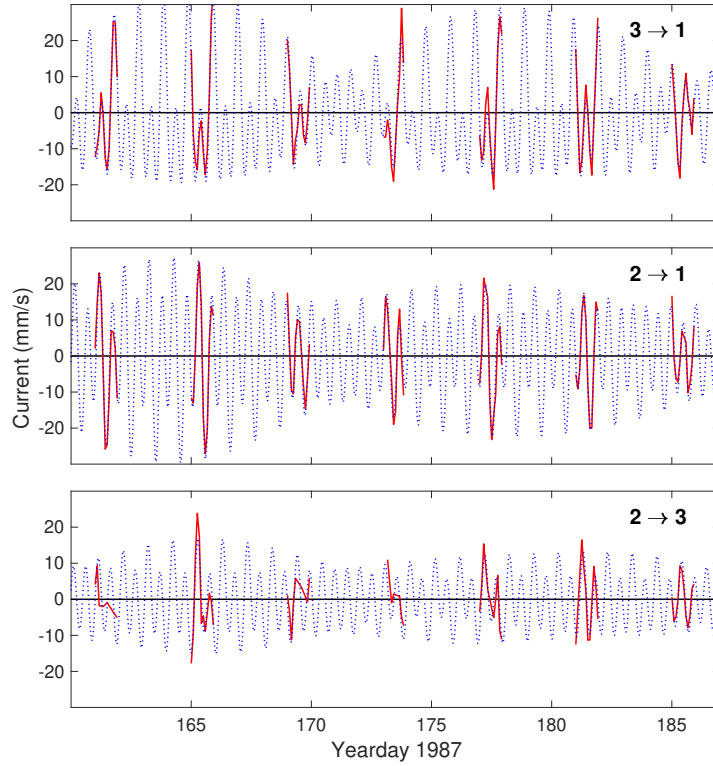


FIG. 4. After removing a daily average, the high-frequency current variations were obtained. Though the time-series are otherwise unfiltered, they show clear tidal variations. A 25-day record length, of about 120 day total, is used to show the tides. The dotted blue line resulted from a tidal analysis of the measurements; the tides account for about 90

was available, and the inverse resolved only barotropic, or depth-averaged, current. Therefore, the inverse estimates for current were depth averaged, resulting in estimated values for barotropic current with uncertainties of about 1 mm/s.

3. Other data

Similar data from the 1991 Acoustic Mid-Ocean Dynamics Experiment (AMODE) in the western North Atlantic (Dushaw 2022a,b) and the 2001 Hawaiian Ocean Mixing Experiment (HOME), north and south of Hawaii (Dushaw 2024c,d,a,b), are available for download.

126 4. Netcdf file contents

127 It may be useful to show a summary of the contents of the netcdf file. The Note gives an
 128 additional set of useful comments. (Lat_1, Lon_1) are the locations of mooring 1, for example.
 129 (yd_m1m2, U_m1m2) are the yearday and barotropic current time series for mooring 1 to mooring
 130 2, of record length Record_Length_m1m2, for example (respecting the sign convention for currents
 131 noted above, U_m1m2 is positive current from mooring 2 to mooring 1, irrespective of the labeling
 132 order of the variable).

133 >> ncdisp(filename)

134

135 Format:

136 netcdf4_classic

137

138 Variables:

139 Experiment

140 Size: 1x68

141 Dimensions: texty1, textx1

142 Datatype: char

143 Note

144 Size: 14x112

145 Dimensions: texty, textx

146 Datatype: char

147 Year

148 Size: 1x1

149 Dimensions:

150 Datatype: double

151 Lat_1

Lat_2

Lat_3

152 Size: 1x1

Size: 1x1

Size: 1x1

153 Dimensions:

Dimensions:

Dimensions:

154 Datatype: double

Datatype: double

Datatype: double

155 Lon_1

Lon_2

Lon_3

156 Size: 1x1

Size: 1x1

Size: 1x1

157 Dimensions:

Dimensions:

Dimensions:

158	Datatype: double	Datatype: double	Datatype: double
159			
160			
161	yd_m1m2	yd_m1m3	yd_m2m3
162	Size: 253x1	Size: 337x1	Size: 186x1
163	Dimensions: N12	Dimensions: N13	Dimensions: N23
164	Datatype: double	Datatype: double	Datatype: double
165	U_m1m2	U_m1m3	U_m2m3
166	Size: 253x1	Size: 337x1	Size: 186x1
167	Dimensions: N12	Dimensions: N13	Dimensions: N23
168	Datatype: double	Datatype: double	Datatype: double
169	Record_Length_m1m2	Record_Length_m1m3	Record_Length_m2m3
170	Size: 1x12	Size: 1x12	Size: 1x12
171	Dimensions: rly,rlx	Dimensions: rly,rlx	Dimensions: rly,rlx
172	Datatype: char	Datatype: char	Datatype: char

173 5. Acknowledgements

174 This work was supported by National Science Foundation grants OCE-82-14918 and OCE-84-
175 14978 and Office of Naval Research contracts N00014-80-C-0217, N0014-84-G-0214, N0014-87-
176 K-0120, N0014-87-K-0760.

177 References

178 Dushaw, B. D., 2015a: An Empirical Global Model for Mode-1 Internal Tides (1.1) [Data set].
179 *Zenodo*, <https://doi.org/10.5281/zenodo.18726454>.

180 Dushaw, B. D., 2015b: An empirical model for mode-1 internal tides derived from satellite
181 altimetry: Computing accurate tidal predictions at arbitrary points over the world oceans. Tech.
182 Rep. Technical Memorandum TM 1-15, Applied Physics Laboratory, University of Washington,
183 Seattle, WA, 114 pp. URL http://www.apl.washington.edu/project/project.php?id=tm_1-15.

184 Dushaw, B. D., 2022a: Acoustic Mid-Ocean Dynamics Experiment (AMODE), 1991,
185 North Atlantic: High-frequency Baroclinic Mode-1 Amplitudes. *Zenodo.org*, URL
186 <https://zenodo.org/record/6662719#.Yq7E9zXMIUc>, <https://doi.org/10.5281/zenodo.6662719>.

187 Dushaw, B. D., 2022b: Acoustic Mid-Ocean Dynamics Experiment (AMODE),
 188 1991, North Atlantic: High-frequency Barotropic Currents. Zenodo.org, URL
 189 <https://zenodo.org/record/6659034#.Yq7EUDXMIUc>, [https://doi.org/10.5281/zenodo.](https://doi.org/10.5281/zenodo.6659034)
 190 6659034.

191 Dushaw, B. D., 2024a: The 2001 Hawaiian Ocean Mixing Experiment (HOME):
 192 High-frequency (>1cpd) Barotropic Current Data from the Northern Tomographic Array. Zen-
 193 odo.org, URL <https://zenodo.org/record/12590519#.Yq7E9zXMIUc>, [https://doi.org/10.5281/](https://doi.org/10.5281/zenodo.12590519)
 194 zenodo.12590519.

195 Dushaw, B. D., 2024b: The 2001 Hawaiian Ocean Mixing Experiment (HOME):
 196 High-frequency (>1cpd) Barotropic Current Data from the Southern Tomographic Array. Zen-
 197 odo.org, URL <https://zenodo.org/record/12590584#.Yq7EUDXMIUc>, [https://doi.org/10.5281/](https://doi.org/10.5281/zenodo.12590584)
 198 zenodo.12590584.

199 Dushaw, B. D., 2024c: The 2001 Hawaiian Ocean Mixing Experiment (HOME):
 200 Mode-1 Internal-tide Amplitude Data from the Northern Tomographic Array. Zenodo.org,
 201 URL <https://zenodo.org/record/12590033#.Yq7E9zXMIUc>, [https://doi.org/10.5281/zenodo.](https://doi.org/10.5281/zenodo.12590033)
 202 12590033.

203 Dushaw, B. D., 2024d: The 2001 Hawaiian Ocean Mixing Experiment (HOME):
 204 Mode-1 Internal-tide Amplitude Data from the Southern Tomographic Array. Zenodo.org,
 205 URL <https://zenodo.org/record/12590217#.Yq7EUDXMIUc>, [https://doi.org/10.5281/zenodo.](https://doi.org/10.5281/zenodo.12590217)
 206 12590217.

207 Dushaw, B. D., 2026a: The 1987 Reciprocal Tomography Experiment (RTE):
 208 Barotropic Current Data from the Triangular Tomographic Array. Zenodo.org, URL
 209 <https://zenodo.org/record/20535627#.Yq7EUDXMIUc>, [https://doi.org/10.5281/zenodozenodo.](https://doi.org/10.5281/zenodozenodo.20535627)
 210 20535627.

211 Dushaw, B. D., 2026b: The 1987 Reciprocal Tomography Experiment (RTE):
 212 Internal-tide Mode-1 Amplitude Data from the Triangular Tomographic. Zenodo.org,
 213 URL <https://zenodo.org/record/20535997#.Yq7EUDXMIUc>, [https://doi.org/10.5281/zenodo.](https://doi.org/10.5281/zenodo.20535997)
 214 20535997.

215 Dushaw, B. D., G. D. Egbert, P. F. Worcester, B. D. Cornuelle, B. M. Howe, and K. Metzger, 1997:
 216 A TOPEX/POSEIDON global tidal model (TPXO.2) and barotropic tidal currents determined
 217 from long-range acoustic transmissions. *Prog. Oceanogr.*, **40**, 337–367, [https://doi.org/10.1016/](https://doi.org/10.1016/S0079-6611(98)00008-1)
 218 S0079-6611(98)00008-1.

219 Dushaw, B. D., and D. Menemenlis, 2023: Resonant diurnal internal tides in the North At-
 220 lantic: 2. modeling. *Geophysical Research Letters*, **50**, e2022GL101193, [https://doi.org/](https://doi.org/10.1029/2022GL101193)
 221 10.1029/2022GL101193.

222 Dushaw, B. D., and P. F. Worcester, 1998: Resonant diurnal internal tides in the North Atlantic.
 223 *Geophys. Res. Lett.*, **25**, 2189–2192, <https://doi.org/10.1029/98GL01583>.

224 Dushaw, B. D., P. F. Worcester, B. D. Cornuelle, and B. M. Howe, 1994: Barotropic currents and
 225 vorticity in the central North Pacific Ocean during summer 1987 determined from long-range
 226 reciprocal acoustic transmissions. *Journal of Geophysical Research: Oceans*, **99**, 3263–3272,
 227 <https://doi.org/https://doi.org/10.1029/93JC03335>.

228 Dushaw, B. D., P. F. Worcester, B. D. Cornuelle, B. M. Howe, and D. S. Luther, 1995:
 229 Baroclinic and barotropic tides in the central North Pacific Ocean determined from long-
 230 range reciprocal acoustic transmissions. *J. Phys. Oceanogr.*, **(25)**, 631–647, [https://doi.org/](https://doi.org/10.1175/1520-0485(1995)025<0631:BABTIT>2.0.CO;2)
 231 10.1175/1520-0485(1995)025<0631:BABTIT>2.0.CO;2.

232 Dushaw, B. D., P. F. Worcester, and M. A. Dzieciuch, 2011: On the predictability of mode-1
 233 internal tides. *Deep-Sea Res. I*, **(58)**, 677–698, <https://doi.org/10.1016/j.dsr.2011.04.002>.

234 Stammer, D., and Coauthors, 2014: Accuracy assessment of global barotropic ocean tide models.
 235 *Rev. Geophys.*, **52**, 243–282, <https://doi.org/10.1002/2014RG000450>.